ELSEVIER

Biophysical Chemistry 87 (2000) 43–61

Biophysical Chemistry

www.elsevier.nl/locate/bpc

Microscopic model of protein crystal growth

Andrzej M. Kierzek[a], Piotr Pokarowski[b], Piotr Zielenkiewicz[c,*]

[a] *Institute of Biochemistry and Biophysics, Polish Academy of Sciences, Pawińskiego 5a, 02-106 Warsaw, Poland*
[b] *Institute of Mathematics, Polish Academy of Sciences Śniadeckich 8, 00-950 Warsaw, Poland*
[c] *Institute of Biochemistry and Biophysics, Polish Academy of Sciences, Pawińskiego 5a, 02-106 Warsaw, Poland*

Received 23 March 2000; received in revised form 15 June 2000; accepted 15 June 2000

Abstract

A microscopic, reversible model to study protein crystal nucleation and growth is presented. The probability of monomer attachment to the growing crystal was assumed to be proportional to the protein volume fraction and the orientational factor representing the anisotropy of protein molecules. The rate of detachment depended on the free energy of association of the given monomer in the lattice, as calculated from the buried surface area. The proposed algorithm allowed the simulation of the process of crystal growth from free monomers to complexes having 10^5 molecules, i.e. microcrystals with already formed faces. These simulations correctly reproduced the crystal morphology of the chosen model system — the tetragonal lysozyme crystal. We predicted the critical size, after which the growth rate rapidly increased to approximately 50 protein monomers. The major factors determining the protein crystallisation kinetics were the geometry of the protein molecules and the resulting number of kinetics traps on the growth pathway.

Keywords: Protein crystallisation; Lattice simulations; Lysozyme

1. Introduction

The growth of large and well ordered protein crystals remains the major obstacle in protein structure determination by means of X-ray crystallography [1]. One of the reasons is that the protein crystallisation process lacks a physicochemical understanding. Although much has been done for the development of empirical crystallisation protocols [2,3], these protocols would certainly be improved if one could better understand the molecular mechanisms of the crystallisation process.

The first systematic studies of protein crystal growth were reported in the late 1970s. In volume 114 of *Methods in Enzymology* (1984), Kam and Feher [4] summarised the results of early observations of protein crystal growth with the use of

* Corresponding author. Fax: +48-39-12-16-23.
E-mail address: piotr@ibbrain.ibb.waw.pl (P. Zielenkiewicz).

0301-4622/00/$ - see front matter
PII: S0301-4622(00)00179-4

light scattering, arrested nucleation assays and ultraviolet light transmission. Since then, many state-of-the-art experimental techniques have been applied to collect observable studies on protein crystal growth. The growth of crystal faces has been studied by electron microscopy and atomic force microscopy [5–7]. The computerisation of light scattering equipment made it possible to collect important data concerning the early stages of the crystallisation process [8–11]. For the same task, X-ray and neutron scattering techniques were applied [12–14]. Calorimetric studies have been also carried out [15]. Many efforts have been dedicated to the study of the influence of various physical factors on protein crystallisation. The effects of temperature, pressure, electric and magnetic fields have been studied [1,16,17]. Protein crystallisation has been studied in microgravity conditions during several space missions [18].

As the amount of experimental data on protein crystallisation increased, many authors attempted to develop theoretical models for their interpretation. There have been many applications of the classical nucleation theory [4,19]. Various computer simulations have been also performed. To understand the effective interactions controlling charged protein aggregation, the potential of mean force for the lysozyme–water–NaCl system has been computed within a hypernetted chain approximation [20,21]. Wolde and Frenkel [22] modelled the nucleation of protein crystals as the process of critical density fluctuations.

The theories mentioned above have not taken into account the dependence of the free energy of protein–protein association on the complex shapes of the protein molecules. Therefore, they have neglected the well-known fact that associating proteins tend to form interfaces with the largest buried surface area [23]. Also, the orientational effect, i.e. the probability that protein monomers which are close together in space are properly oriented to form a defined interface, is omitted. This simplification influences kinetic results by several orders of magnitude, as the reported values of orientational probabilities vary in the range 10^{-5}–10^{-7} [24–27].

The above simplifications can be avoided if detailed knowledge about the structure of the crystal is used to provide insights into the mechanism of its growth. Using the atomic level structure of the crystal, one can build a model of crystal growth in such a way that the anisotropy of the protein molecules (a general or detailed shape of the protein) is considered. The objective of such an approach is not to predict crystallisation conditions, but to use the knowledge of protein structure to deduce the mechanisms of crystal growth. The prediction of crystallisation conditions seems to be intractable, as the growth units of protein crystals are folded protein chains, and, therefore, the crystallisation process is determined by the structure of the protein. On the contrary, the understanding of the mechanisms of the early stages of protein crystal growth can be useful in designing new crystallisation protocols. For example, knowledge about the size distribution of aggregates during the crystallisation of some model proteins would help to improve protocols for monitoring the process by means of scattering methods. This, in turn, would shorten the necessary time to decide if the protein would crystallise under the given conditions.

In the works briefly reviewed below, the shape of the protein molecules has been used in the computer simulations concerning crystal formation. Very general aspects of protein aggregation were studied by two-dimensional Monte Carlo simulations, in which protein monomers were represented by hexagons, the edges of which modelled surface patches with different properties [28]. Pellegrini et al. [29] performed Monte Carlo simulations in which nuclei were assembled from three-dimensional rigid bodies with different surface patches. They were able to explain the non-uniform distribution of space groups found in the Brookhaven Protein Data Bank [30]. Computer simulations have been used to model the behaviour of the faces of a tetragonal lysozyme crystal [24]. In this work, the interactions on three main types of protein–protein contacts in the crystal were used as the free parameters of the model. Tissen et al. [31] used triangulated surfaces of the model proteins and performed Stokesian dynamics and continuum hydrodynamics calculations. Due to a detailed representation of protein monomers, calculations were time con-

suming, and only results concerning the diffusion coefficients of the proteins under investigation have been reported so far.

In our previous works, we used lattice simulations to study the nucleation and early growth stages of a tetragonal lysozyme crystal [27,32]. The protein molecules were modelled as points occupying the nodes of a three-dimensional lattice. The edges of the lattice represented contacts between protein molecules in the crystal. Contact energies were calculated, assuming that they were proportional to the change of the accessible surface area during the formation of the interface. A discrete orientational state was assigned to each of the monomers in the lattice, and interactions were considered only between molecules which were properly oriented. Such a representation of the system allowed us to use interaction energies, calculated according to the analysis of the crystal structure on the atomic level, to account for orientational effects and, at the same time, to avoid the computational complexity of explicit protein structure treatment during random walk simulations.

One of the simplifications of our simulation that have been presented so far is that it did not allow for the dissociation of the monomers attached to the growing crystal. In this work, a reversible model was formulated. Our original idea of the lattice simulations was used, but the monomers were allowed to dissociate from the crystal surface with a probability depending on their interaction energies. In this work, we have presented computer simulations of the tetragonal lysozyme crystal growth, from free monomers to complexes of 10^5 molecules. These large complexes exhibited the morphology of the macroscopic crystal, which validated the results presented for the early stages of crystal formation. The model was also justified by the fact that it reproduced the experimentally observed behaviour of the steps on the (110) face of the crystal. The computer simulations presented in this paper are, to our knowledge, the first which provide the insights into the kinetic pathways of protein crystal formation from the complexes as small as a few molecules up to the microcrystals with the faces already formed.

2. Formulation of the model

2.1. Random walk simulation

In our model, we have simulated the diffusion of protein molecules in solution as the random walk of points in the three dimensional lattice. At the beginning of the simulation, a defined number of points were assigned to random nodes in the lattice. The ratio of the number of points and the number of nodes in the lattice was equal to the volume fraction of the protein studied under crystallisation conditions. The simulation proceeded as follows: in each time step of the simulation the interaction energy was evaluated for every molecule in the lattice. Each molecule that did not interact with others was randomly moved. During the move, one of the neighbouring nodes of the lattice was chosen randomly. The molecule was moved to this node if it was not occupied by another one. Otherwise, the molecule was not moved in the given timestep. For the molecule that interacted with other ones, it was first questioned if it would detach from the lattice site it occupied. The probability of detachment depends on the interaction energy of the molecule. For the molecule that detached from the lattice site, the move was executed according the same rules as for non-interacting molecules.

The protein molecules which were brought into contact by translational diffusion were usually not properly oriented to form one of the interfaces present in the crystal. The numerical parameter we used to account for this feature was orientational probability. Orientational probability is defined as the probability that the two molecules of the certain shape are aligned in proper orientation to form a defined interface when they meet in space. To implement this parameter in our lattice simulation, we assigned a discrete orientational state (integer variable) to each molecule. The molecules occupying the neighbouring nodes of the lattice were treated as interacting only if they had the same orientational state. The number of orientational states was the reciprocal of orientational probability. At the beginning of the simulation, random orientational states were assigned to molecules. Then, the orientational state

of each molecule was randomly changed whenever this molecule moved.

The distance between neighbouring nodes of the lattice corresponded approximately to the diameter of the protein molecule. Therefore, the timestep of the random walk simulation could be calculated as the time required by the molecule to move a distance equal to its diameter, using the equation for the mean squared displacement of a Brownian particle:

$$\Delta t = \langle (x)^2 \rangle / 6D \quad (1)$$

The mean squared displacement $\langle (x)^2 \rangle$ was assumed to be equal to $4a^2$, where a is the hydrodynamic radius of a molecule. The hydrodynamic radius was used instead of the average radius of a molecule, as determined according to crystal structure. The rationale was that the actual Brownian particle that moves in the solvent is a protein molecule surrounded by a hydration shell.

2.2. Lattice geometry and energy calculations

Atomic level knowledge about the crystal under investigation was incorporated into the random walk simulation in the following way: first the environment of the protein molecule in the crystal under investigation was analysed. The environment was defined as the complex containing the protein monomer, which will be referred to as the central molecule, and all molecules in the crystal, which form with it at least one intermolecular contact shorter than 4.5 Å. For each of the interfaces formed by the central molecule, the free interaction energy was calculated. It was assumed that the interaction free energy was proportional to the change of accessible surface area during the formation of the interface. Details concerning the generation of the crystal environment and energy calculations were given in a previous paper [27].

The lattice that was subsequently used in the simulation was built in such a way that each node, together with its neighbours, represented a cluster of molecules built around the central molecule during the analysis of the crystal environment. In other words, each node represented the position of the molecule in the crystal, and each edge represented one of the intermolecular interfaces found in the crystal environment. Details concerning the co-ordinate system used to implement the lattice were given in a previous paper [27].

The free association energy of the kth monomer in the lattice $\Delta G^0_{\text{assoc}}(k)$ could be calculated using the following equation:

$$\Delta G^0_{\text{assoc}}(k) = \Sigma \delta(k,j) \Delta G^0_{\text{inter}}(j) \quad (2)$$

where $\delta(k,j) = 1$ if the jth neighbouring node of molecule k is occupied by a monomer with the same orientational state as k, and is $= 0$ otherwise; $\Delta G^0_{\text{inter}}(j)$ is interaction free energy between the central molecule and its jth neighbour in the crystal environment. Fig. 1 shows the schemes of the lattice and random walk simulations.

2.3. Probability of detachment

In order to perform the random walk simulation, we needed to calculate the probability $p-$ that, in the given timesteps of the simulation, the molecule breaks the interactions which it forms with other molecules in the system.

Let us consider all the molecules in the system which, in the given timestep, had association free energies equal to E. In the next iteration of the simulation, n_{E^-} of them detached from the nodes they occupied, while n remained attached. We assumed that in the early stages of crystal growth the concentration of the free monomers did not change significantly. Therefore, we could use the mean values of n_{E^-} and n:$\langle n_{E^-} \rangle$, $\langle n \rangle$. The ratio of $\langle n_{E^-} \rangle$ and $\langle n \rangle$ is given by the following equation:

$$\langle n_{E^-}/n \rangle = \Theta \exp(-E/\mathrm{RT}) \quad (3)$$

where Θ is the equilibrium value of $\langle n_{E^-}/n \rangle$, T is absolute temperature and R is a gas constant. The probability $p^-(E)$ that a given molecule with free association energy E would detach from the lattice node it occupies is equal:

$$p^-(E) = \langle n_{E^-}/(n + n_{E^-}) \rangle \quad (4)$$

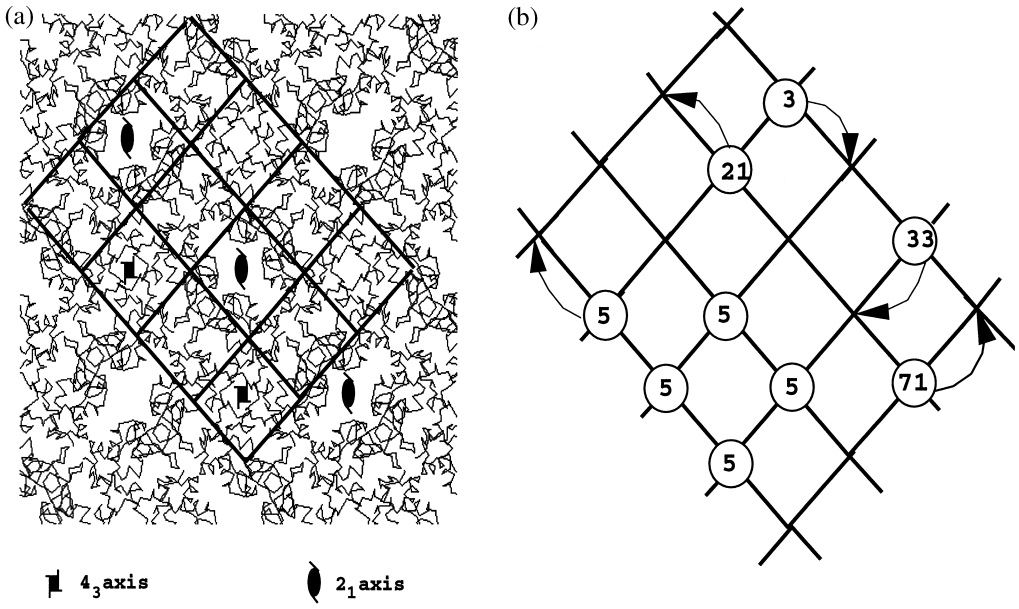

Fig. 1. Schemes of the random walk simulation. (a) A two-dimensional slice of the tetragonal lysozyme crystal perpendicular to the *c* direction. Part of the lattice built according to the analysis of the crystal structure is shown. The node of the lattice represents the position of the monomer; the edges represent intermolecular interfaces. (b) During the simulation, monomers were represented as points occupying the nodes of the lattice. A discrete orientational state was assigned to each monomer in order to account for the anisotropy of protein molecules. The reciprocal of the number of orientational states will be referred to as orientational probability. If monomers occupy neighbouring nodes and have the same orientational states, they form an interface. Thus, the molecules with orientational states 3 and 21 do not interact, despite their occupation of neighbouring nodes. For each monomer its interaction free energy is calculated as the sum of the interaction energies pre-calculated for the interfaces it forms with other molecules. The arrows show movement of molecules in the time step of simulation. Each molecule can move with a probability depending on its interaction free energy. Molecules belonging to the compact tetramer shown in the picture move with a much lower probability than other molecules.

which can also be written as:

$$p^{-}(E) = \langle n_{E^-}/n \; 1/(1 + n_{E^-}/n) \rangle$$

After the substitution of Eq. (3) into Eq. (4) we have:

$$p^{-}(E) = \Theta \exp(-E/\mathrm{RT})/[1 + \Theta \exp(-E/\mathrm{RT})] \quad (5)$$

In the random walk model of diffusion, the probability p^{+} that the molecule will attach at a the given position in the lattice in the given timestep can be approximated as the product of the volume fraction of the molecules *c* (the ratio of the numbers of occupied and free lattice nodes) and the orientational probability P_O:

$$p^{+} = P_O c \quad (6)$$

By considering the probability p^{+} as equal for all lattice nodes, we neglected the fact that some nodes can have different diffusion accessibilities due to the occupation of neighbouring nodes. In the case of low orientational probabilities, this simplification did not significantly influence the results.

The equilibrium condition for the crystal was frequently written as the equality between the rate of attachment at the equilibrium concentration and the rate of detachment from the so-called half crystal site [33,34,24]. In the fcc lattice, the layer of growth units could be deposited on the surface, or removed from the surface by attachment/detachment, only at kink sites which had

an energy equal to exactly half of the energy of the site having all neighbouring nodes occupied. Therefore, if the rate of attachment at the kink site was equal to the rate of detachment from it, then the whole crystal could be dismantled or assembled without a free energy cost. This satisfied the principle of microscopic reversibility at equilibrium [35]. In our model, the equilibrium condition formulated in this way became:

$$P_O s = p^-(\Phi) \tag{7}$$

where s is the equilibrium concentration of monomers and Φ is the energy of the half crystal site. After the substitution of Eq. (5) into Eq. (7), one can obtain the expression for Θ:

$$\Theta = P_O s/(1 - P_O s)\exp(\Theta/\mathrm{RT}) \tag{8}$$

Thus $p^-(E)$ can be written as:

$$p^-(E) = \gamma \exp[(\Phi - E)/\mathrm{RT}]/[1 + \gamma \exp(\Phi - \mathrm{E})/\mathrm{RT})] \tag{9}$$

where $\gamma = P_O s/(1-P_O s)$.

In the tetragonal lysozyme crystal, the model system in our study, there was a particular problem concerning the half-crystal site energy. Both the (110) and (101) faces present in the macroscopic crystal could not be dismantled by removing molecules which had half of their bonds free. Additionally, it was impossible to dismantle the faces by removing only molecules with the same bonding pattern. Therefore, the half-crystal site, as defined in the classic models [33], could not be found in the tetragonal lysozyme crystal.

In spite of the lack of the half-crystal site, the parameter Φ could be used in the model as the mean free association energy of the molecules removed from the crystal on the pathways on which it was dismantled at equilibrium state. We did not attempt to find these pathways by means of geometrical considerations, as it would require a detailed analysis of the edge effects in the macroscopic crystal. Instead of doing this, we treated Φ as the free parameter of the model.

2.4. Parameters of the model

Two parameters of the model, the probability of detachment and the energy of kink sites, must be set according to agreement with experimental data. In the case of a tetragonal lysozyme crystal, this could be done by a simulation of the behaviour of the step on the (110) face of the crystal, which has been observed with molecular resolution by atomic force microscopy (AFM). According to AFM experiments, the (110) face grew by a movement of the steps which were two molecules high. The speed of the moving step could also be estimated from the pictures taken over time intervals.

At the beginning of the simulation, we built the (110) crystal face in the simulation box. On top of the face we placed an additional two layers of the molecules, forming the step. To the free nodes of the lattice we randomly assigned monomers (see Fig. 2). The number of monomers was set to reproduce the protein concentration of 5 mg/ml used by Konnert et al. [6] in their AFM experiments. A detailed protocol of this simulation is given in the caption to Fig. 2.

We observed that, by varying energy of kink site, we influenced the geometry of the growing face. If the value of Φ was high (approx. 20 kcal/mol) the step and the crystal face dissolved. For low values of Φ (approx. 10 kcal/mol), the face grew by the attachment of the molecules to all sites on the face rather than by attachment only at the edge of the step. For $\Phi = 15 \pm 2$ kcal/mol, the face grew by the movement of the step — in agreement with experimental data.

The orientational probability did not influence the geometry of the growing face, but determined the speed of the movement of the step. According to the AFM pictures made by Konnert et al. [6] over 1-min intervals, the speed of the step was equal to 0.3 μm/min. A random walk simulation reproduced this value to within the order of magnitude (0.48 μm/min) if the orientational probability was set to 10^{-5}.

2.5. Fast algorithm of crystal growth simulation

For very low values of orientational probability,

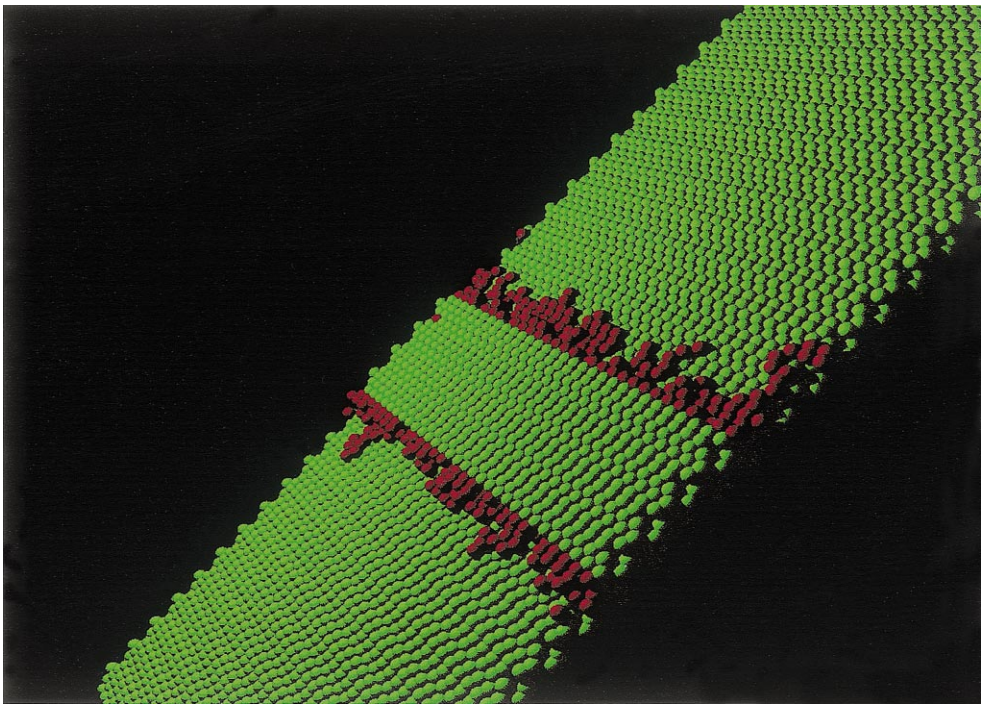

Fig. 2. Movement of the step on the (110) face of the tetragonal lysozyme crystal. A random walk simulation was performed in the lattice of the size $30 \times 30 \times 30$ unit cells. A (110) face of the size 30×30 unit cells, built from the two layers of molecules was put into the lattice. An additional two layers of molecules were placed on top, thus forming a step of size 4×30 molecules. These are represented by green spheres. The nodes 'below' the face were also filled with molecules. This left 103 440 nodes of the lattice free. To this free volume, 860 molecules were added in random positions (volume fraction 0.008 as used by Konnert et al. in AFM experiment [6]). The periodic boundary conditions in the lattice were set in such a way that each node on the boundary face of the simulation box was connected by the edge lying in the same plane parallel to the (110) one on the other side of the simulation box. Forty-seven million random walk steps were executed. The molecules that attached to the growing face and remained attached for 10 000 steps are represented by red spheres. Whenever such a molecule was detected, a new one was added to the system in order to keep the concentration of free monomers constant. At the end of simulation (configuration shown on the picture) 300 molecules were found to be attached to the face. The edges of the step moved, on average, by 107 Å. When this is divided by the time of simulation the resulting speed of the moving step is 0.48 μm/min.

most of the collisions did not result in the formation of the specific interactions. Therefore, before any aggregate was formed in random walk simulations, a very large number of iterations needed to be executed. This made the algorithm highly time-consuming. In practice, only the attachment of a few hundred molecules to a formed crystal face could be simulated. Any calculations concerning the early stages of growth were impossible.

We developed an algorithm, equivalent to the random walk, which allowed the simulation of single microcrystal growth from the size of a few monomers up to a size of more than 10^5 monomers. It was assumed that each nucleus of the ordered phase present in the solution grew independently of others, i.e. that the aggregation of microcrystals and competition for monomers did not play a role in the early stages of crystal growth.

At the beginning of the simulation, the initial complex was put into the lattice and the time of the simulation was set to 0. Then, all the sites were found. Each site was processed in the following way: the appearance of a properly oriented monomer in a site in the given random walk step

was considered as the success of a Bernoulli trial with probability p^+. Therefore, the number of random walk steps one should wait for the attachment of the monomer to the site had a geometric distribution with parameter p^+:

$$P(t=k) = p^+(1-p^+)^k \quad \text{where } k = 0,1,... \qquad (10)$$

For each of the sites, the time of attachment of a monomer at this site was calculated as a random number from the above distribution. The value of p^+ was calculated as the product of the volume fraction of the system and orientational probability (Eq. (6)).

After the examination of all sites, the molecules

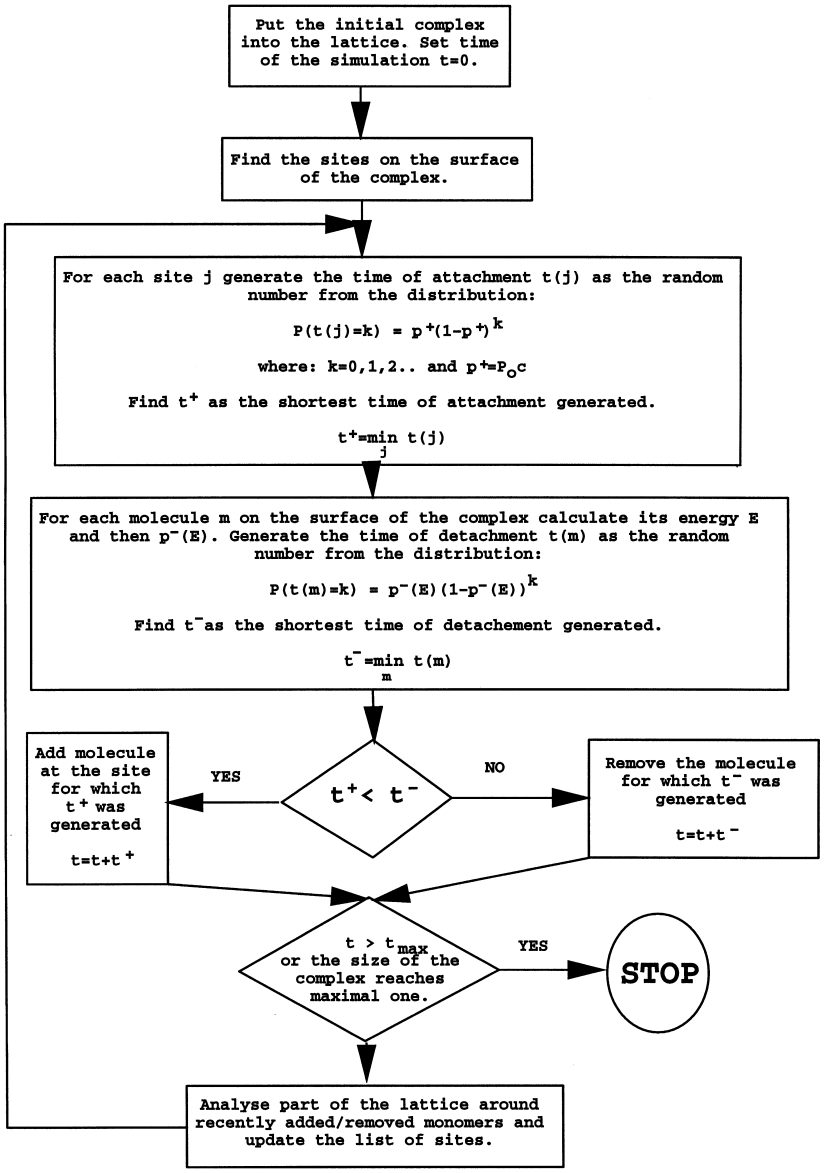

Fig. 3. Flowchart of the fast algorithm.

which have at least one unoccupied neighbouring node were examined in order to consider their possible dissociation. For each of them, the free energy of association (Eq. (1)) and corresponding p^-(Eq. (9)) were calculated. The dissociation of the molecule in the given time step of the simulation was treated as the success of a Bernoulli trial with probability p^-. Therefore, for each molecule exposed on the surface of the growing complex, the time of its detachment was generated as a random number from geometric distribution with probability p^-.

Finally, the shortest time of all — the generated attachment and detachment time — was found. If it was an attachment time, the molecule was added at the site for which it was generated. If the shortest time was generated for one of the surface molecules, then that molecule was removed from the complex. The complex grew or dissolved by iteration of the above steps. A flowchart of the simulation is shown in Fig. 3.

In order to test if the fast algorithm of growth was equivalent to the random walk one, we applied the new algorithm to the simulations of the movement of a step. As the initial complex, we used the fragment of the face shown on Fig. 2. The volume fraction of monomers, their equilibrium concentration, Φ, and orientational probability were set to the same values as in the case of the random walk simulation. The qualitative results of the application of the fast algorithm were the same as the results of random walk simulation — the face grown by the movement of the step. The speed of the step was 0.82 μm/min.

We believed that the agreement within the order of magnitude (compared to many orders of magnitude on both the scales of time and size of the protein crystallisation process) between the results of the simulations with both algorithms and the experimental value was sufficient to conclude that the fast algorithm of crystal growth was both equivalent to the random walk algorithm and reproduced the experimentally determined speed of the step moving on the (110) face of the crystal.

2.6. Generation of the initial complex

In an ideal case, we would like to obtain a small ordered complex by the random walk simulation and then subject it to the growth simulation by the fast algorithm. Unfortunately, there was still a 'gap' between these two algorithms. For an orientational probability of 10^{-5}, it was impossible to obtain complexes larger than three molecules in the random walk simulation. If the trimer was used as the initial complex in the fast algorithm simulation, it immediately dissolved. We performed a large number (of the order of 10^8) of growth simulations using dimers and trimers as initial complexes. In all cases, the small complexes completely dissolved in the simulations and microcrystals never appeared. We believe that the reason for this was that the appearance of a growing crystal is an event occurring with a very low probability. In order to observe a growing crystal, one should examine a very large number of the small complexes. This number is beyond the reach of computer resources. Fortunately, it was possible to find a few of the large number of possible pathways leading from dimers to macroscopic crystals using the following hierarchical procedure:

1. Fast algorithm simulations starting from dimers were performed. Each simulation used one of the eight possible dimers as the initial complex. A large number of the simulations were executed. The largest size of the complex obtained during all these simulations was found. All of the complexes that grew to this size were recorded, together with their time of growth.
2. The complexes recorded in the previous step were used as the initial ones in the next ensemble of fast algorithm simulations. Again, the largest complexes and times of their growth were recorded.
3. The simulations in point 2 were iterated until the complexes which were able to grow into macroscopic crystals were obtained.

For each iteration of the above protocol, the fraction of the initial complexes which grew to the maximal size could be calculated. Using these fractions, and the concentration of dimers calculated from the random walk simulation, one could estimate the timescale of the appearance of the

Table 1
Surface areas and association free energies of the protein–protein interfaces found in tetragonal lysozyme crystal

Letter code of the interface	Surface area buried in the interface [A^2]	Calculated interaction free energy (kcal/mol)
a	37.5	−0.3
b	37.5	−0.3
c	548.5	−6.0
d	341.3	−3.8
e	341.3	−3.8
f	548.5	−6.0
g	1104.4	−10.95
h	657.0	−8.25

complex which grew to a macroscopic crystal. A detailed formulation of the 'hierarchical' calculations is given in Appendix A.

3. Application of the model and results

All the calculations were performed for the tetragonal lysozyme crystal. The crystal environment was generated using co-ordinates stored in the 5LYZ entry [36] of the protein data bank. There were eight interfaces in the crystal environment. The accessible surface areas, and interaction energies calculated for these interfaces, are listed in Table 1. The volume fraction in all the simulations was set to 0.037, which was shown by Eberstein et al. [8] to be optimal for lysozyme crystallisation in 0.54 M NaCl and 0.1 M acetate buffer (pH 4.2). The equilibrium concentration of monomers was set to the solubility of the lysozyme, which was 0.005 [5]; Φ was equal 15 kcal/mol and the orientational probability was set to 10^{-5}. The values of the diffusion constant D (102 $\mu m\ s^{-1}$) of lysozyme and the corresponding hydrodynamic radius a (2.09 nm) were taken from Eberstein et al. [8]. The timestep of the simulations, calculated according to Eq. (1), was 28 ns.

3.1. Morphology of the growing microcrystals and geometry of the faces

Firstly, we performed simulations of the formation of first ordered complexes using an iterative approach. In the first iteration, dimers were used as initial complexes and the maximal size of the complexes was 5 molecules. In the following iteration, pentamers were used as initial complexes and heptamers were obtained. The heptamers were able to grow to decamers and decamers to 100-mers. All complexes of a size of 100 molecules were able to grow to the limit of computer resources (approx. 10^5 monomers). The results of these simulations are summarised in the Table 2.

We chose one of the complexes of a size of 100 molecules, which had been previously obtained, and used it as the initial complex in the growth simulation. The simulation was stopped when the complex reached the size of 120 000 monomers. This complex is shown in Fig. 4. As can be seen,

Table 2
Results of the iterative simulation protocol

Initial and maximal size of the complex used in the calculations	Number of initial complexes subjected to growth by fast algorithm	Number of the complexes with the maximal size obtained	Time of growth from initial complex to the complex with maximal size [timesteps]
2, 5	10^9	8	35 041
5, 7	2.5×10^6	29	2.14×10^9
7, 10	78 000	49	2.02×10^8
10, 100	2×10^6	7	2.35×10^9

Fig. 4

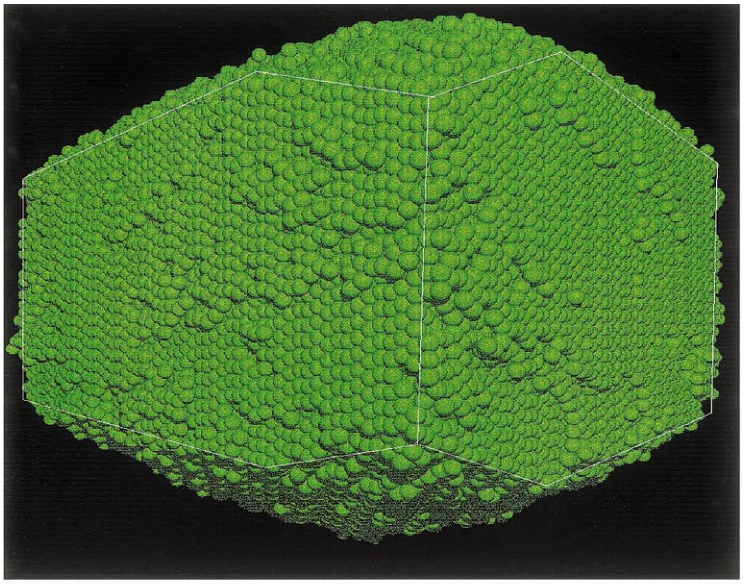

Fig. 5

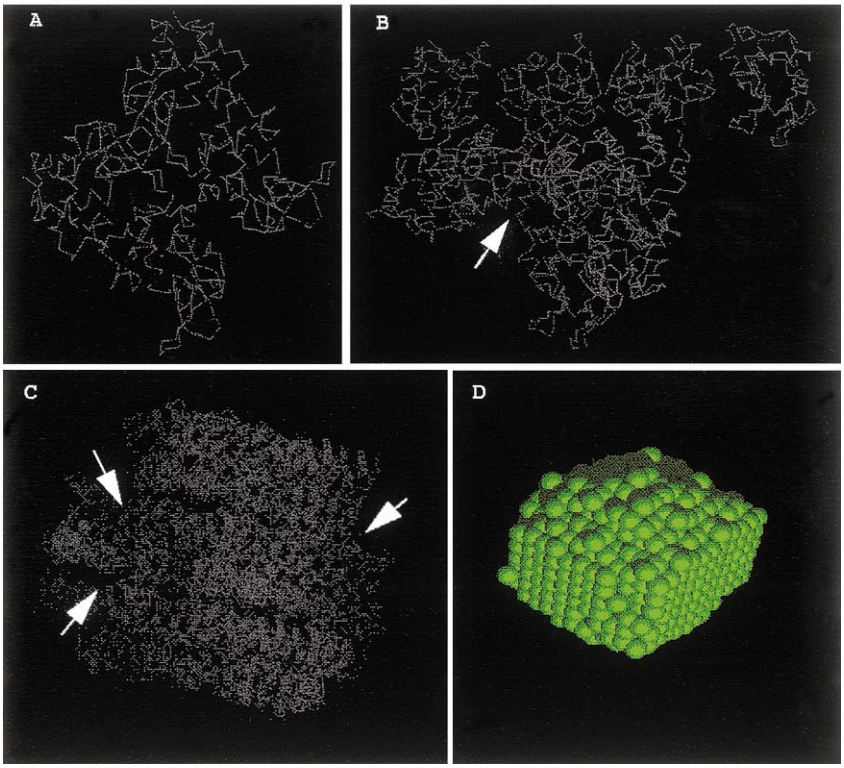

Fig. 4. A microcrystal of the size of 120 000 monomers. The edges of (110) faces are marked on the picture. These faces grow by the movement of the steps, as observed experimentally.

Fig. 5. The complexes of the size 4, 10, 100, 1000 monomers (pictures A, B, C, D, respectively) found on the growth pathway of the microcrystal shown on Fig. 4. Arrows mark good sites.

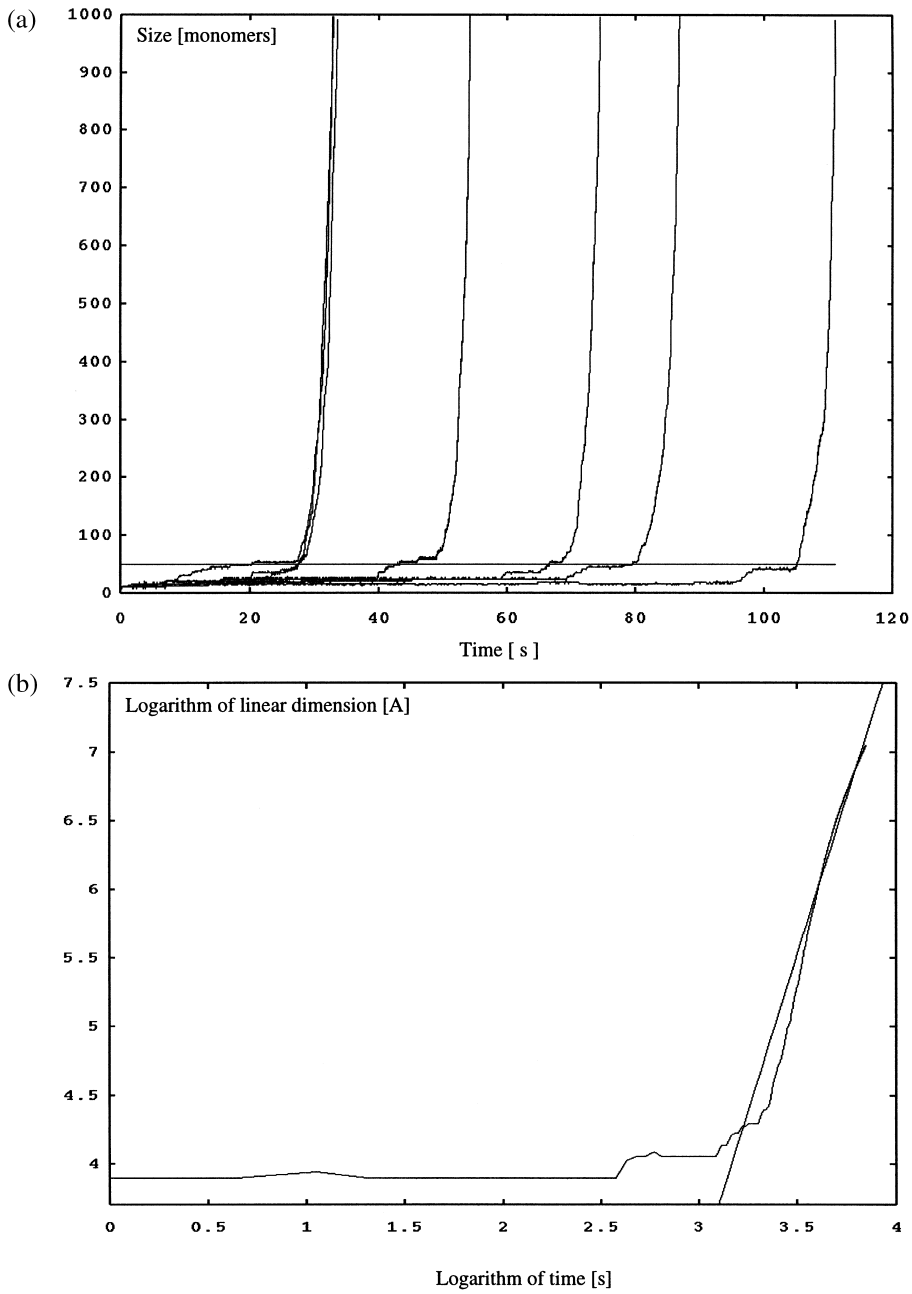

Fig. 6. Growth trajectories obtained in the simulations. (a) Seven microcrystals that were able to grow to a size larger than 100 molecules. Critical size of approximately 50 molecules is shown. (b) One of the complexes presented on A has been grown to the size of 120 000 molecules. Growth trajectory obtained in this simulation is shown on the log–log scale. The part of the curve corresponding to complexes larger than 100 monomers can be fitted with the function $y = 4.567 \times - 10.442$.

the microcrystal had (110) faces already formed. The beginning of the formation of (101) faces could also be seen. The (110) faces grew by the movement of the steps. Most of the steps had one-layer structures, although two molecules high steps were also present.

3.2. Geometry of the small complexes

We examined the geometry of the complexes which were present on the growth pathway of the microcrystal shown on Fig. 4. Fig. 5 shows complexes of sizes of 4, 10, 100 and 1000 molecules. The tetramer shown in the picture was a part of all the pentamers obtained in our calculations. The complex of size 10 molecules was one of the 10-mers obtained in the calculations. The complex of size 100 molecules was used as the initial one in the simulation of microcrystal growth, and the complex of size 1000 molecules was present in the growth pathway obtained in this simulation. All of the complexes were compact in the sense that most of the molecules formed more than one interface with other molecules in the complex.

The arrows in the pictures mark several sites on the surfaces of the complexes. As can be seen, a molecule which arrived at one of these sites would have a large part of its surface area buried in the interfaces with other molecules. Therefore, its free interaction energy would be high and the dissociation probability low. Let us refer to the sites shown on the pictures as good sites.

It is obvious that crystal growth is much more probable at good sites than by the attachment of molecules which formed only single interfaces with the complex, such as one of the molecules belonging to the 10-mer shown in Fig. 5. This molecule will dissociate unless another one attaches close to it, and forms an interface with it and the rest of the complex. If this happens, the two molecules would bury large surface area in their interfaces to provide a free interaction energy, significantly decreasing their dissociation probability.

As can be seen in Fig. 5, the tetramer did not contain any good sites. The complex of size 10 molecules was sufficiently large to contain a few of them; the 100-molecule large complex contained many more. The complex of 1000 molecules had its (110) faces already formed. Close to the edge of two (110) faces, there were structures resembling the steps which would later form. The edges of the steps contained good sites.

3.3. Timescales for the formation of the first ordered complexes

We performed a random walk simulation of 8000 monomers in a lattice of size $30 \times 30 \times 30$ unit cells (volume fraction = 0.037). At the beginning of the simulation, all the monomers were put into random positions of the lattice. After 2.2×10^6 timesteps, the largest complexes observed in the lattice were trimers. The mean waiting time for the appearance of a trimer was 19 728 timesteps. The number of dimers oscillated around a value of 30 ± 5. This corresponded to a concentration of 7.7 mM.

Using the equations given in Appendix A and the results shown in the Table 2 one could estimate the mean waiting time for the appearance of a dimer which would grow to macroscopic crystal. For a volume of 0.1 ml, the result was 9.34×10^6 timesteps, which corresponded to 0.3 s. The mean time of growth from a dimer to a complex of size 100 molecules was 4.7×10^7 timesteps, which corresponded to 131 s.

3.4. Growth curves of microcrystals

For each of the microcrystals of size 100 molecules, obtained with the iterative approach (see Table 2), we simulated growth up to a size of 1000 monomers. Fig. 6 shows the growth curves obtained in these simulations. Three of the curves were almost the same. The remaining four represented slower growth trajectories. As can be seen, each growth trajectory was composed of two parts. The microcrystals grew slowly until they reached a certain critical size, and then they quickly reached a size of 1000 molecules. The critical size was approximately 50 monomers, and did not vary significantly among growth curves. The time of growth to the critical size varied between 20 and 100 s.

For the growth curve obtained in the simula-

tion which was stopped at a size of 120 000 monomers, we generated a log–log plot of the linear dimension of the crystal vs. time. The linear dimension was calculated as:

$$l = (kV)^{1/3} \quad (11)$$

where k is the number of the molecules in the complex and V is the volume of the sphere of radius equal to the hydrodynamical radius of lysozyme (9129.33 Å^3). The part of the curve corresponding to complexes of sizes greater than 100 molecules could be fitted with a linear relationship with a slope of 4.567 and intercept of -10.442 (correlation coefficient = 0.98). According to this relationship, the crystal reached a linear dimension of 1 mm after 334 s.

4. Discussion

4.1. Scenario of the early stages of lysozyme crystal growth

In this section, the mechanism governing the formation of the tetragonal lysozyme crystal has been formulated according to the results of our simulations. The scenario of events presented here concerns the early stages of the formation of a crystal. The phenomena occurring in a solution containing macroscopic crystals, such as the cessation of growth, cannot be directly studied by the theory presented in this work.

The theory predicted that the growth unit of the tetragonal lysozyme crystal was a monomer. In the solution of lysozyme, the dimers were formed first. The lifetime of these dimers was of the order of 10^{-4} s, and their concentration is approximately 8 μM. Only one dimer per 10^9 grew into a complex of a size larger than 100 molecules. All of the growth trajectories leading from the dimer to large complexes contained the tetramer shown in Fig. 5. The tetramer was compact, and due to this fact, a molecule arriving at one of its sites was only able to form a single contact. Any single crystal interface had too low a free interaction energy to stabilise the monomer in the lattice. Therefore, a molecule attached to the complex by a single contact would dissociate, unless, in a very short time, another properly oriented molecule arrived in a neighbouring site. If this happened, the two molecules would form a compact aggregate on the surface of the complex. A large surface area was buried in the interface formed between the molecules and their interfaces with the complex, which implied high interaction energy and low dissociation probability. To be more specific, the probability of attachment of another molecule close to the two previously attached was higher than the probability of their dissociation from the surface. Therefore, the further growth of the tetramer required that two properly oriented molecules arrive in neighbouring sites in a short period of time. It is convenient to refer to such an event as the surface aggregation of two molecules. The complexes that were larger than the tetramer and required surface aggregation could also appear. Due to a very low orientational probability, the appearance of two properly oriented monomers in the neighbouring sites in the short period of time was very unlikely. Therefore, the appearance of a complex which required the surface aggregation of two molecules significantly decreased the speed of growth on the given growth trajectory. In the case of very small complexes, of less than 10 monomers, it usually caused the full dissociation of the already-formed complex. A particular growth trajectory, obtained in the simulation, could be considered as one of a large number of kinetic pathways of the crystallisation process. Complexes which were compact and required surface aggregation in order to grow could be treated as kinetic traps.

When the complex reached a size of approximately 50 molecules, its growth rate rapidly increased. This was caused by the fact that the complex contained sites which were able to incorporate single molecules. In other words, there were no longer any kinetic traps on the pathway. Another effect which caused an increase of the speed of growth was the increase of the surface area of the complex. As the complex grew, the number of sites on its surface increased. The probability of attachment of a molecule to the complex, and also the probability of surface aggregation, increased with the number of sites.

This, in turn, decreased the mean waiting time for the attachment of molecules and increased the growth rate. The time scale of growth of the complexes smaller than 50 molecules was governed by kinetic traps. The rate of growth of a complex larger than 50 molecules was determined by the number of sites. Therefore, both the mechanism and time scales of growth were different for complexes smaller and larger than 50 molecules. Thus, a size of approximately 50 molecules could be considered as critical.

According to the simulations, a dimer, which subsequently grew to a complex larger than the critical size, appeared in a volume of 1 ml of solution approximately every 0.03 s. The growth of the dimer to a size of 50 molecules took 20–100 s. Therefore, in a volume of 0.1 ml, the first complex of a critical size was expected to appear after approximately 1 min. Then, after each 0.3 s, another complex of this size appeared. The waiting time for the appearance of a dimer that grew to a critical size increased linearly as the volume decreased. The time of growth of a particular complex did not depend on the volume. As shown in Fig. 6, the growth from the critical size to the maximal size used in the simulations was much faster. The time of growth from a critical size to a macroscopic one was estimated as being approximately 5 min. This result should be taken with care, as it was obtained by the extrapolation of the growth curve rather than the direct application of the model. It also concerns the time and size scales at which the effects, not accounted for by the model, can occur. These effects are, e.g. the cessation of growth and competition for monomers.

It was assumed that, in the early stages of crystal growth, all the microcrystals grew independently, i.e. that their aggregation and competition for monomers did not play a significant role in the process. This assumption was supported by the results of the simulation, which showed that the concentration of the microcrystals was so low that there was no point in considering their aggregation. The number of dimers present in solution was two orders of magnitude lower than the number of monomers. It is obvious, therefore, that the tetramer was formed by the surface aggregation of two monomers on a dimer rather than by the aggregation of two dimers. The aggregation of larger complexes need not be considered, as their concentration was even lower than that of the dimers. Complexes of a size not larger than 10^5, which was the limit in our simulations, were also unable to significantly decrease the number of monomers present in the solution. We concluded, therefore, that in the timescales of the simulations, the complexes grew independently. The competition for monomers certainly occurred when the crystals were of macroscopic sizes (approx. 10^{15}) monomers.

The (110) faces were first observed in a complex of the size of 1000 molecules, shown in Fig. 5D. The (101) faces could only be seen in complexes close to the maximal size used in our simulation i.e. 120 000 molecules. The (110) face grew by the movement of steps.

The results of this work implied that a major factor influencing the crystallisation kinetics of the proteins was the anisotropy of protein molecules. At very early stages of the process, compact complexes frequently become kinetic traps due to low value of orientational probability. For a system in which the orientational probability is higher, the effect of the requirement for surface aggregation would not be so dramatic. Therefore, one can see that even under 'ideal' crystallisation conditions, proteins crystallise slowly because they are highly anisotropic.

The number of compact complexes which are kinetic traps on crystallisation pathways of the given crystal depends on the geometry of the protein molecule and the crystal order. Thus, different crystals of different proteins can have different numbers of crystallisation pathways, which quickly lead from small complexes to macroscopic crystals. One could expect, therefore, that some proteins could crystallise more easily than others due to geometrical constraints, or even exhibit different shapes of growth curve.

4.2. Comparison with experimental data

The largest microcrystal obtained in our simulations showed many features that were in agreement with the observables collected for macro-

scopic crystals. The faces observed in the tetragonal lysozyme crystal were present. The (110) face grew by the movement of the steps, as shown by atomic force and electron microscopy. The shape of the crystal resulting from our model was in agreement with light microscopy data.

The morphology of the crystal faces formed in the simulations was, of course, strongly determined by the assumed order of the lattice and the fact that the simulation of (110) face was used to find the value of Φ. On the contrary, the shape of the crystal was determined by intermolecular interactions rather than by crystal order [37]. Therefore, the shape of the crystal presented in Fig. 5 supported the application of the interaction energies, calculated according to the Eisenberg and McLachlan approach [38].

One should note at this point that the prediction of crystal order and morphology was not the goal of this paper. In this work, we used the knowledge of the structure of the model protein crystal to propose the mechanism of the early stages of its formation, which cannot be observed experimentally. Therefore, the fact that growth simulations started from complexes as small as dimers led to the formation of the complex exhibiting properties of macroscopic crystal, strongly supports our conclusions.

In 1997, Janin [24] calculated the orientational probability for the Barnase–Barstar system according to experimental data of Schreiber and Ferscht [39]. The result of 1.5×10^{-5} was in agreement with the value of 10^{-5} obtained in this work. The fact that two independent analyses of different experimental data gave the same order of magnitude of orientational probability supports this estimation.

There are two discrepancies from experimental data that need to be commented on here. Firstly, the simulation predicted that the steps on the (110) face were one molecular layer high, although the some of them were two layers high, as observed by AFM. This can be corrected by a minor modification of interaction energies. We simulated the growth of the complex of a size of 120 000 molecules using the following values of the interaction energies: −0.3, −0.3, −6.592, −4.392, −4.392, −6.592, −10.358, and −7.066 for the interfaces a, b, c, d, e, f and g, respectively (see Table 1). None of the energies were changed by more than 2 kT (1.184 kcal/mol at 295 K). In this simulation, more steps of two molecules high appeared on the (110) face of the crystal. The shape of the crystal and the timescale and mechanism of its early growth stages did not change.

The second discrepancy, with respect to the experimental data, was the very short time of the appearance of the macroscopic crystals. The model predicted that, in the volume range used in the experiments, the first crystal should appear after approximately 5 min. This contradicts laboratory experience that macroscopic crystals are rarely observed before 24 h. On the other hand, the shortest time of the appearance of the lysozyme crystals, as reported in literature, was as short as a fraction of 1 h [4]. Therefore, taking into account the fact that the timestep of the simulation was nine orders of magnitude lower than the timescale of the appearance of macroscopic crystal, we believe that discrepancy reported above does not falsify our conclusions concerning the early stages of the crystallisation process.

The results of the model showed, that after the appearance of the first macroscopic crystal, the next appear in the timescale of 0.3 s in a volume of 0.1 ml. This time is definitely too short if one takes into account that usually only a few macroscopic crystals are observed in the solution, even after weeks of crystal growth. This results from the fact that our simulations only considered the early stages of the crystallisation process. The presence of macroscopic crystals significantly depleted the number of monomers present in the solution. Therefore, the number of crystals observed after a few days was the result of competition between them. According to the model, competition between the crystals started in the first hour of crystallisation, as the simulations suggested the presence of macroscopic crystals in this timescale. The phenomena occurring in the timescales when the large crystals are present in the solution, such as cessation of growth and competition for monomers, will be the subject of future research.

There is debate in the literature concerning the

nature of the growth unit of tetragonal lysozyme crystal. Nadarajah et al. [40] have claimed that the speed of the growth of the (110) face, measured as the function of supersaturation can be reproduced only by models assuming an aggregate growth unit. The growth unit predicted by the authors was the octamer, which was part of the 4_3 helix. In an earlier work, Durbin and Feher [24] proposed a model of the growth of the crystal faces that was able to reproduce the supersaturation dependence of the speed of growth, assuming a monomer growth unit. As stated above, our model predicted that aggregates appeared in too low populations to become growth units in the crystal. In our opinion, the strongest evidence against aggregate growth unit was also provided by AFM and electron microscopy observations of the growing (110) face. Both techniques clearly showed that the lower layer of molecules, on the edge of the two-molecule high step was extended with respect to the upper one. The models assuming tetramer and octamer growth units did not reproduce these observations, as they assumed an attachment of the units which were already two molecules high. The edge of the step formed by such units would be also two molecules high with both layers of equal length. In contrast, our model (see Fig. 4) and the work of Durbin and Feher [24], predicted that the lower layer of monomers was extended with respect to the upper one. In both models the two-layer structure was the result of different energies of the molecular contacts formed on the surfaces of the layers.

We concluded that the results of our simulations were in agreement with experimental data concerning the morphology and habit of macroscopic crystals. The estimation of orientational probability — the parameter that determines the timescale of growth — was validated by independent estimation. This allowed us to believe in the results concerning the very early stages of crystallisation, which could not be observed experimentally.

5. Conclusions

The results of this work have shown that the major factor which determines protein crystallisation kinetics is the geometry of protein molecules. The magnitude of the speed of crystal growth is determined by a very low orientational probability, resulting from the anisotropy of protein molecules. Due to geometrical constraints, many of the smallest complexes with a crystal order do not have sites which are able to incorporate single molecules, and their further growth requires the surface aggregation of two molecules. These complexes become kinetic traps on crystallisation pathways as surface aggregation is, due to low orientational probability, many orders of magnitude slower than the incorporation of a single molecule. All complexes that are larger than the critical size are able to incorporate single molecules. The size of the critical complex is also the result of geometrical constraints. Therefore, the simulations presented in this work show that protein crystal growth is difficult, not only because it is difficult to find the proper crystallisation conditions, as even under ideal crystallisation conditions proteins do not easily crystallise because they are highly anisotropic.

This work has shown computer simulations of the tetragonal lysozyme crystal formation. The theory used for these simulations was formulated in such a way that it was also applicable for other protein crystals. The study of the possible diversity of protein crystallisation mechanisms will be the subject of future research.

Acknowledgements

We are grateful to Dr Y. Georgalis for critical comments on the manuscript. A.K. acknowledges financial support of Foundation for Polish Science.

Appendix A

In order to find kinetic pathways leading from dimers to macroscopic crystals, and to estimate the timescales of the appearance of the complexes on these pathways, the following simulation protocol was executed:

1. An ensemble of $n_{sim}(2)$ fast algorithm simulations with an initial complex of size 2 molecules were executed. In each simulation, the initial complex was generated randomly as the one of the eight possible dimers. Each simulation was carried out until the size of the complex decreased to a monomer or a complex of size $s(2)$ was obtained. Each complex of size $s(2)$, together with its time of growth, was recorded. Let $n(2)$ denote the number of these complexes. The average time of growth $t_{gr}(2)$ from a dimer to a complex of size s was calculated.
2. An ensemble of $n_{sim}(j)$ fast algorithm simulations with initial complexes of the size $j = s(2)$ were executed. For each simulation, the initial complex was taken randomly from the $n(2)$ complexes recorded in the previous step. The simulation was carried out until the complex completely dissolved or reached the size $s(j)$. Complexes of size $s(j)$ were recorded together with their times of growth. The number $n(j)$ of complexes reaching the size $s(j)$, and the average time of growth $t_{gr}(j)$ from a complex of size $s(2)$ to a complex of size $s(j)$, were calculated.
3. The simulations in point 2 were iterated until complexes of size s_{max} were obtained. The size s_{max} was set in such a way that all complexes of a size exceeding s_{max} were able to grow up to the limit of computer resources.

For each ensemble of growth simulations, the fraction $f(j)$ of the complexes which reached the size of $s(j)$ molecules was calculated as:

$$f(j) = n(j)/n_{sim}(j) \tag{12}$$

The fraction of dimers formed in the solution which reached the size s_{max} was calculated as the product of the fractions $f(j)$.

In the random walk simulation, the number of dimers present in the lattice oscillated around a constant value. Let $N(V)$ denote the mean number of dimers present in the volume V of any timestep of the simulation. The fraction F of the dimers present in solution in the timestep of the simulation which would lead to the formation of a complex of the size s_{max} is given by the equation:

$$F = N(V) \times \prod f(j) \tag{13}$$

Therefore, for a volume V, the mean waiting time t_d for the appearance of a dimer which would grow to the complex of the size s_{max} is the reciprocal of the fraction F:

$$t_d = 1/F \tag{14}$$

The sum of the mean times of growth $t_{gr}(j)$ recorded in the calculations is the mean time of growth of a particular dimer to a complex of the size s_{max}:

$$t_s = \Sigma t_{gr}(j) \tag{15}$$

Therefore, the first complex of size s_{max} is expected to appear in the solution after $t_d + t_s$ timesteps of the simulation. Afterwards, such a complex appears every t_d timesteps.

References

[1] S.D. Durbin, G. Feher, Protein crystallization, Annu. Rev. Phys. Chem. 47 (1996) 171–204.
[2] C. Carter, Response surface methods for optimising and improving reproducibility of crystal growth, Methods Enzymol. 276 (1997) 74–99.
[3] I. Rayment, Reductive alkylation of lysine residues to alter crystallization properties of proteins, Methods Enzymol. 276 (1997) 171–179.
[4] Z. Kam, G. Feher, Nucleation and growth of protein crystals: general principles and assays, Methods Enzymol. 114 (1984) 77–112.
[5] S.D. Durbin, G. Feher, Studies of crystal growth mechanism of proteins by electron microscopy, J. Mol. Biol. 212 (1990) 763–774.
[6] J.H. Konnert, P.D. Antonio, K.B. Ward, Observation of growth steps, spiral dislocations and molecular packing on the surface of lysozyme crystals with the atomic force microscope, Acta Cryst. D50 (1994) 603–613.
[7] A.J. Malkin, Yu.G. Kuznetsov, T.A. Land, J.J. DeYoreo, A. McPherson, Mechanisms of growth for protein and virus crystals, Nat. Struct. Biol. 2 (1995) 956–959.
[8] W. Eberstein, Y. Georgalis, W. Saenger, Molecular interactions in crystallizing lysozyme solutions studied by photon correlation spectroscopy, J. Cryst. Growth 143 (1994) 71–78.

[9] A.J. Malkin, A. McPherson, Light-scattering investigations of nucleation processes and kinetics of crystallization in macromolecular systems, Acta Cryst. D50 (1994) 385–395.
[10] A. Schaper, Y. Georgalis, P. Umbach, J. Raptis, W. Saenger, Precrystallization structures in supersaturated lysozyme solutions studied by dynamic light scattering and scanning force microscopy, J. Chem. Phys. 106 (1977) 8587–8594.
[11] P. Umbach, Y. Georgalis, W. Saenger, Time-resolved small angle static light scattering on lysozyme during nucleation and growth, J. Am. Chem. Soc. 120 (1998) 2382–2390.
[12] N. Niimura, Y. Minezaki, M. Ataka, T. Katsura, Aggregation in supersaturated lysozyme solution studied by time-resolved small-angle neutron scattering, J. Cryst. Growth 154 (1995) 136–142.
[13] Y. Georgalis, J. Schuler, J. Frank, D.M. Soumpasis, W. Saenger, Protein crystallization screening through scattering techniques, Adv. Colloid Interface Sci. 58 (1995) 57–75.
[14] O.D. Velev, E.W. Kaler, A.M. Lenhoff, Protein interactions in solution characterized by light and neutron scattering. Comparison of lysozyme and chymotrypsinogen, Biophys. J. 75 (1998) 2682–2697.
[15] Y. Georgalis, P. Umbach, A. Zielenkiewicz et al., Microcalorimetric and small-angle light scattering studies on nucleating lysozyme solutions, J. Am. Chem. Soc 119 (1997) 11959–11965.
[16] D.M. Blow, N.E. Chayen, L.F. Lloyd, E. Saridakis, Control of nucleation of protein crystals, Prot. Sci. 3 (1994) 1638–1643.
[17] N.I. Wakayama, Quantitative study of crystallisation kinetics of hen egg-white lysozyme using magnetic orientation, J. Cryst. Growth 191 (1998) 199–205.
[18] S. Koszelak, J. Day, C. Leja, R. Cudney, A. McPherson, Protein and virus crystal growth on international microgravity laboratory 2, Biophys. J. 69 (1995) 13–19.
[19] Y. Bessho, M. Ataka, M. Asai, T. Katsura, Analysis of the crystallization kinetics of lysozyme using a model with polynuclear growth mechanism, Biophys. J. 66 (1994) 310–313.
[20] M.D. Soumpasis, Y. Georgalis, Potential of mean force treatment of salt mediated protein crystallization, Biophys. J. 72 (1997) 2770–2774.
[21] Y. Georgalis, P. Umbach, M.D. Soumpasis, W. Saenger, Dynamics and microstructure formation during nucleation of lysozyme solutions, J. Am. Chem. Soc. 120 (1998) 5539–5548.
[22] P.R. Wolde, D. Frenkel, Enhancement of protein crystal nucleation by critical density fluctuations, Science 277 (1997) 1975–1978.
[23] C. Chothia, J. Janin, Principles of protein–protein recognition, Nature 256 (1975) 705–708.
[24] S.D. Durbin, G. Feher, Simulation of lysozyme crystal growth by the Monte Carlo method, J. Cryst. Growth 110 (1991) 41–51.
[25] S.H. Northrup, H.P. Erickson, Kinetics of protein–protein association explained by Brownian dynamics computer simulations, Proc. Natl. Acad. Sci. USA 89 (1992) 3338–3342.
[26] J. Janin, The kinetics of protein–protein recognition, Proteins 28 (1997) 153–161.
[27] A.M. Kierzek, W.M. Wolf, P. Zielenkiewicz, Simulations of nucleation and early growth stages of protein crystals, Biophys. J. 73 (1997) 571–580.
[28] S.Y. Patro, T.M. Przybycien, Simulations of reversible protein aggregate and crystal structure, Biophys. J. 70 (1996) 2888–2902.
[29] M. Pellegrini, W.S. Wukovitz, T.O. Yeates, Simulation of protein crystal nucleation, Proteins 28 (1997) 515–521.
[30] F.C. Bernstein, T.F. Koetzle, G.J.B. Williams, E.F. Meyer Jr., M.D. Brice, The protein data bank: a computer-based archival file for macromolecular structures, J. Mol. Biol. 112 (1977) 535–542.
[31] J.T.W.M. Tissen, J. Drenth, H.J.C. Berendsen, J.G.E.M. Fraaije, Simulation of protein crystallization. I.: Static calculation, Biophys. J. 67 (1994) 1801–1805.
[32] A.M. Kierzek, P. Pokarowski, P. Zielenkiewicz, Lattice simulations of protein crystal formation, Biophys. Chem. 77 (1999) 123–137.
[33] G.H. Gilmer, Computer models of crystal growth, Science 208 (1980) 355–363.
[34] R. Xiao, J.I.D. Alexander, F. Rosenberger, Morphological evolution of growing crystals: a Monte Carlo simulation, Phys. Rev. A43 (6) (1991) 2447–2456.
[35] K. Laidler, Chemical Kinetics, Third Edition, Harper Collins Publishers, 1987, p. 129.
[36] R. Diamond, D.C. Phillips, C.C.F. Blake, A.C.T. North, Real-space refinement of the structure of hen egg-white lysozyme, J. Mol. Biol. 82 (1974) 371–382.
[37] C. Hammond, The Basics of Crystallography and Diffraction, Oxford University Press, 1997.
[38] D. Eisenberg, A.D. McLachlan, Solvation energy in protein folding and binding, Nature 319 (1986) 199–203.
[39] G. Schreiber, A. Fersht, Rapid, electrostatically assisted association of proteins, Nat. Struct. Biol. 3 (1996) 427–431.
[40] A. Nadarajah, L. Meirong, M.L. Pusey, Growth mechanism of the (110) face of the tetragonal lysozyme crystals, Acta Cryst. D53 (1997) 524–534.